Published in final edited form as:
Mol Imaging. 2009 ; 8(1): 45–54.

Near-Infrared Imaging of Injured Tissue in Living Subjects using IR-820

Suresh I Prajapati[1,*], **Carlo O Martinez**[2,*], **Ali N Bahadur**[1], **Isabel Q Wu**[1], **Wei Zheng**[3], **James D Lechleiter**[3], **Linda M McManus**[4,5], **Gary B Chisholm**[7], **Joel E Michalek**[7], **Paula K Shireman**[2,6,9], and **Charles Keller**[1,3,8]

[1]Greehey Children's Cancer Research Institute, San Antonio, TX 78229 USA

[2]Department of Surgery at the University of Texas Health Science Center, San Antonio, TX 78229 USA

[3]Department of Cellular & Structural Biology at The University of Texas Health Science Center, San Antonio, TX 78229 USA

[4]Department of Pathology at The University of Texas Health Science Center, San Antonio, TX 78229 USA

[5]Department of Peridontics at The University of Texas Health Science Center, San Antonio, TX 78229 USA

[6]Department of Medicine at The University of Texas Health Science Center, San Antonio, TX 78229 USA

[7]Department of Epidemiology & Biostatistics at The University of Texas Health Science Center, San Antonio, TX 78229 USA

[8]Department of Pediatrics at The University of Texas Health Science Center, San Antonio, TX 78229 USA

[9]The South Texas Veterans Health Care Systems, San Antonio, TX 78229 USA

Abstract

The unprecedented increase in pre-clinical studies necessitates high-throughput, inexpensive and straightforward methods for evaluating diseased tissues. Near-infrared imaging of live subjects is a versatile, cost-effective technology that can be effectively used in a variety of pathological conditions. We have characterized an inexpensive optoelectronic chemical, IR-820, as an infrared blood pool contrast agent to detect and quantify diseased tissue in live animals. IR-820 has maximal excitation and emission wavelengths of 710 nm and 820 nm, respectively. IR-820 emission is significantly improved *in vivo* upon serum binding to albumin and elimination occurs predominantly via the gastrointestinal tract. We demonstrate the utility of this contrast agent for serially imaging of traumatized tissue (muscle), tissue following re-perfusion (*e.g.* stroke) and tumors. IR-820 can also be employed to map regional lymph nodes. This novel contrast agent is anticipated to be a useful and an inexpensive tool for screening a wide variety of preclinical models of human diseases.

Corresponding author: Charles Keller, MD, 8403 Floyd Curl Drive, MC-7784, San Antonio, TX 78229-3900, Office: (210) 562-9062; Fax: (210) 562-9014, kellerc2@uthscsa.edu.
* These authors contributed equally

COMPETING INTERESTS STATEMENT
Use of IR-820 as a preclinical/clinical contrast agent is under intellectual property evaluation by UTHSCSA.

Keywords

IR-820; biomarker; optical imaging; muscle injury; near-infrared contrast agent

Introduction

Serial live imaging is emerging as an important part of preclinical studies. Among imaging modalities, optical imaging is becoming one of the most versatile and informative methodologies, especially when coupled with contrast agents. Near-infrared (NIR) contrast agents are ideally suited to live animal studies due to the deep tissue penetration and reduced light scattering1. Classically, NIR blood pool contrast agents have been used in retinal angiography2, and for clinical determination of cardiac output3 and hepatic function4. Clinical NIR contrast agents, such as Indocyanine Green, have also been used in preclinical development. Other similarly effective but more costly blood pool contrast agents have been developed specifically for preclinical use5, 6. NIR optical imaging takes advantage of the "Window of Transparency" between 700-900 nm, where light absorption is at a minimum in tissue along with comparatively lower scattering. These characteristics allow NIR light to travel >1.5 cm in tissue before being completely absorbed7. Herein we describe a novel, inexpensive blood pool contrast agent and its use in differentiating between normal and diseased tissue in live animals using NIR fluorescence imaging.

Methods

Contrast agent

The commercially available optoelectronic chemical IR-820 ($C_{46}H_{50}ClN_2NaO_6S_2$) was purchased from Sigma-Aldrich (catalog# 543365, St. Louis, MO). IR-820 has a molecular weight of 849.47 atomic mass units (amu) and is normally used as a laser and near-infrared dye. For each experiment, the powdered IR-820 was freshly mixed with phosphate buffer saline (PBS) to a final concentration of 0.2 mM and 100 μl of this solution was used for injecting into experimental animals.

Optical imaging protocol

The Xenogen IVIS® Spectrum system (Caliper – Xenogen, Alameda, CA) was used to capture images for all experiments. The instrument employs a scientific grade, cryogenically cooled CCD camera which has a low-noise, 16 bit digitized electronic readout. All images were acquired using the epi-illumination method at excitation wavelength of 710 nm and emission wavelength of 820 nm unless otherwise stated. The camera settings were kept constant at 1 sec exposure time, 2×2 binning, 12.6 cm field of view, and f/stop of 1/2. The data was acquired and analyzed using the manufacturer's Living Image 3.2© software.

Excitation and emission spectra

To determine the excitation and emission spectra for IR-820, the solution was loaded into a clean cuvette and was imaged after 15 minutes. The images were acquired using a set of excitations ranging from 435-745 nm (windows of 35 nm) and emission filters ranging from 500-840 nm (windows of 20 nm).

Protein interaction with IR-820

To determine the relative size of serum proteins that bind IR-820, serum-IR-820 samples were separated on a 10% SDS polyacrylamide gel, stained with Coomassie Blue and imaged.

In vivo pharmacokinetics of IR-820

All animal procedures were conducted in accordance with the Guidelines for the Care and Use of Laboratory Animals and were approved by the Institutional Animal Care and Use Committee (IACUC) at University of Texas Health Science Center at San Antonio and The South Texas Veterans Health Care System. For pharmacokinetics analysis 2 groups of four *Hairless* $^{SKH1/SKH1}$ mice were used. The first group was injected with IR-820 by intravenous tail vein injection while the second was injected intraperitoneally. Both groups were serially imaged for 8 days. Throughout this study unless otherwise stated, animals were imaged using the same anesthesia protocol, 2% isoflurane in 100% oxygen at 2.5 liters per minute. Body temperature was maintained at 37°C by a heated stage.

Response to increased vascular permeability

For vascular permeability experiments, the skin overlying the dorsal ribcage of a female C57BL/6 mouse (Taconic, Hudson, NY) was shaved three days prior to the imaging experiment. Vascular permeability was increased by intradermal injection of 50 μl of histamine (10 nM and 500 mM) diluted in PBS using a 30 gauge needle on to the dorsal surface of the mouse with histamine or PBS. After 10 minutes, IR-820 was administered by intravenous injection as described above. An area on the dorsal side that did not receive any injection was used to determine the baseline fluorescence. Imaging was performed in triplicate on a single mouse 30 minutes after histamine injection.

Muscle injury model using cardiotoxin (CTX)

Hairless $^{SKH1/SKH1}$ mice were bred at the University of Texas Health Science Center; the original breeders for this colony were obtained from Charles River Laboratories (Wilmington, MA). Twelve week old female mice received intramuscular injections to the anterior compartment muscles below the knee of the right hind limb with either 100 μl CTX (2.5 μM, Calbiochem, San Diego, CA) to induce myonecrosis or normal saline (NS) injections to control for the needle trauma caused by the injection, the left hind limbs in these animals served as non-injected controls.

To determine the kinetics of IR-820 imaging in injured muscle, three groups of mice underwent baseline imaging. Each mouse received an intraperitoneal injection of IR-820 and was imaged 30 minutes later. Immediately after the imaging, the mice received right anterior compartment injections of CTX, NS or no injections (non-injured), n=3-4 mice/group. The mice were serially imaged at 1, 2, and 6 hours post-CTX or NS injection with daily imaging thereafter for 8 days.

To assess for ongoing vascular leak, an additional group of mice received two CTX injections into the anterior compartment of the right hind limb and similar volumes of NS into the anterior compartment of the left hind limb after baseline imaging, n=2 mice. Twenty-four hours after CTX and NS injection, the mice were imaged and received an intraperitoneal injection of IR-820. The mice were serially imaged at 1, 2, and 6 hours after IR-820 injection with daily imaging for 6 days.

A separate group of mice received CTX injection and were euthanized 1 hr, 3 days, and 7 days after CTX injection for histology studies, n=1-2 mice/time point. Bilateral anterior compartment muscles were removed *en bloc*, fixed in 10% neutral buffered formalin, paraffin-embedded and processed by routine histological procedures.

Statistical analysis

To determine whether the fluorescence intensities are dose-dependent, student's t-test was performed using EXCEL™ on the total flux values obtained from all four sites in vascular permeability experiment (Figure 1E).

SAS software (SAS, Cary, NC) was used for all statistical analyses related to muscle injury experiment. Results from corresponding time points of each group were averaged and used to calculate descriptive statistics (mean ± standard deviation). All statistical testing was two-sided with a significance level of 5%.

The absolute value or paired differences of the serially measured signal intensities were compared between treatments or to baseline using the Hochberg step-up Bonferroni method to adjust the p-values produced by repeated measures mixed model contrasts.

In vivo tumor imaging

A mixed strain wild type mouse with a spontaneous neck tumor was injected with IR-820 by tail vein injection and imaged after fifteen minutes. The animal was euthanized and tumor tissue was collected for histology.

Lymph node mapping

To map ipsilateral lymph nodes, a rhabdomyosarcoma-prone transgenic *Myf6* $^{ICNm/WT}$ *Pax3* $^{P3Fm/P3Fm}$ *Trp53* $^{F2\text{-}10/WT}$ *Rb1* $^{Flox/Flox}$ mouse with a foot tumor was injected with IR-820 via a direct intra-tumoral injection. The animal was serially imaged for 2 days. On the second day, the animal was euthanized and tumor sample was collected for analysis including histology.

Rose Bengal induced-cortical photothrombosis model

All animal procedures were conducted in accordance with the Guidelines for the Care and Use of Laboratory Animals (NIH Publication No 85–23, revised 1996) and were approved by the Institutional Animal Care and Use Committee (IACUC) at University of Texas Health Science Center at San Antonio. Male FVB/NJ mice (Jackson Laboratory, Bar Harbor, ME) 6-8 weeks old were initially anesthetized at 4% isoflurane with 100% oxygen and subsequently maintained at 1.5% isoflurane through a nosecone. Depth of anesthesia was monitored by pinch withdrawal and whisker movement. Body temperature was maintained at 37 °C by a feedback-controlled heating pad. The mouse hair was trimmed and a small incision was made in the scalp to expose the skull. A custom-made stainless steel plate was glued to the bone with VetBond Tissue Adhesive (3M, St. Paul, MN). To facilitate photoactivation, a thin cranial window (~2 mm in diameter) was created over the right primary somatosensory cortex (~1.5 mm posterior to Bregma and 2 mm lateral from midline) using a variable-speed electric drill (Fine Science Tools, Foster City, CA). Normal rat ringer (NRR) solution was periodically added to the skull to avoid damage to the underlying cortex or pial vessels by friction-induced heat. Mice were given a 0.1 ml tail-vein injection of 20 mg/ml of photosensitizer Rose Bengal (Sigma, St. Louis, MO) in phosphate buffered saline (PBS) with 25 μg/ml IR-820 (Sigma, St. Louis, MO). Photothrombotic clotting was induced by exposing the cortex under the thinned cranial window to a 543 nm laser for 15 minutes using a 0.8-NA 40× water-immersion objective (Nikon, Melville, NY) to activate Rose Bengal over a 1 mm^2 circular area. After clotting, the plate was detached from the skull, the scalp was sutured, and the mice were carefully monitored until they recovered from anesthesia. The mice were returned to cages for subsequent non-invasive near-infrared fluorescent imaging.

Results

IR-820 is a blood pool contrast agent

IR-820 is an optoelectronic agent used in laser dye applications (Figure 1A Inset). Peak excitation and emission wavelengths were measured to be 710 nm and 820 nm, respectively (Figure 1A). In preliminary experiments we observed that IR-820 fluorescence increased significantly when in contact with biological tissue or serum. To determine whether the increased signal emission was a result of a simple interaction or a biochemical conversion, we measured emissions in the presence of mouse or bovine serum types treated with or without heat inactivation. The serum-bound samples showed consistently higher fluorescence intensity than the signal from unbound IR-820 (data not shown). Heat inactivation did not lead to a decreased signal, suggesting binding was not a complex quaternary complex. To determine which proteins bind IR-820, serum-bound IR-820 samples were electrophoresed on an SDS polyacrylamide gel and imaged for near-infrared fluorescence (Figure 1B). A single 65kDa band was detected; similar results were obtained when IR-820 was incubated with purified bovine serum albumin (Figure 1B).

Pharmacokinetics of IR-820 clearance

The pharmacokinetics of IR-820 by intravenous or intraperitoneal injection was studied *in vivo* using 2 groups of *Hairless*$^{SKH1/SKH1}$ mice (Figure 1C). This strain harbors a PCR-detectable retroviral interruption of the gene *Hr*, rendering the animal fur-free by 30 days of life8. Depending upon the route of administration, the fluorescence signal intensity steadily increased and peaked 48 hours after intravenous injection (Figure 1D) or 6 hours after intraperitoneal injections (Figure 1D). Fecal and urinary excretions were collected daily and imaged, showing that the elimination of IR-820 was hepatobiliary (data not shown). Animals were monitored for 6 weeks after IR-820 administration without any overt signs of toxicity.

IR-820 is sequestered in areas of increased vascular permeability

To determine whether IR-820 would accumulate in tissue with increased vascular permeability, we used intradermal histamine diphosphate salt, an agent known to increase vascular permeability9, to evaluate IR-820 sequestration in a C57BL/6 mouse. The animal's skin was partially shaved and injected at different sites with 10 nM and 500mM histamine, phosphate buffer saline (PBS) and no injection (Figure 1E). Dose-dependent increased fluorescence ($p<0.017$) was observed at the 10 nM and 500 mM injection sites (Figure 1F), confirming that IR-820 was sequestered in tissue manifesting capillary leak.

IR-820 can be used to monitor the time course of capillary leak and recovery following muscle injury

A well-characterized cardiotoxin (CTX) model10 was used to determine the efficacy of IR-820 in monitoring muscle injury. CTX or normal saline (NS) as a control was injected intramuscularly into the anterior compartment of the right hind limb muscles of *Hairless*$^{SKH1/SKH1}$ mice. Normal muscle tissue morphology predominated in NS-injected specimen (Figure 2A). However, within 1 hour after CTX injection, significant microscopic alterations were observed. Myofibers were disrupted, appearing intensely eosinophilic and separated by a protein-rich, acellular material (Figure 2B). Three days following CTX-induced injury, a widespread mononuclear cell inflammatory infiltrate prevailed within and around necrotic myofibers (Figure 2C). Inflamed and necrotic tissue was largely replaced within 7 days by small, regenerated myofibers with centrally-located nuclei. Interspersed adipocytes were also present (Figure 2D).

Imaging was performed on 3 groups of *Hairless*$^{SKH1/SKH1}$ mice receiving intramuscular injections of CTX (Figure 2E), NS or no injection (non-injured group) into the right hind limb anterior compartment 30 minutes after IR-820 injection; the left hind limb served as non-injected control for each animal in all three groups. To determine if CTX or NS injection in the right hind limb altered the kinetics of IR-820 distribution or induced a systemic vascular leak, the signal intensities of the non-injected (left) hind limbs were measured and compared in the three groups (Figure 3A). The non-injured group demonstrated a minimally decreased signal intensity compared to both the CTX and NS groups ($p=0.03$ and <0.001 respectively) at the 6.5 hour time point and an increased signal intensity compared to the NS group ($p\leq0.001$) at the 72 hour time point. Despite these minor differences, the signal intensities were remarkably similar with the peak of IR-820 signal occurring at 6-24 hours, suggesting IR-820-bound albumin remained in the intravascular space in the non-injected left hind limbs in all three groups. The time course of IR-820 signal was similar in the non-injected left hind limbs (Figure 3A) to previous pharmacokinetics experiments measuring total body signal intensity after i.p. injection of IR-820 (Figure 1D).

To determine the extent of injury-induced IR-820 leak into the extravascular space, the signal intensity of the right and left hind limb regions were measured and the paired difference of the injected (right) hind limb signal intensity to the non-injected (left) hind limb signal intensity was calculated (Figure 3B). As expected for the non-injured group (IR-820 i.p. only) the paired difference remained near 0 throughout the study reflecting a similar IR-820 signal in both hind limbs and no significant variation in the paired difference time point values compared to baseline, defined as the paired difference 0.5 hours after IR-820 injection. In contrast, NS injection resulted in a paired difference peak at the 1.5 hour and 2.5 hour time points ($p=0.004$ and 0.01 respectively, compared to non-injured) that quickly decreased to baseline and remained similar to the paired differences derived from the non-injured mice thereafter; significant elevations compared to baseline occurred at the 1.5 to 6.5 hour time points ($p\leq0.002$). With CTX injection, an immediate increase in the paired difference occurred at the 1.5 hour time point representing an increased extravascular IR-820 signal in the injected hind limb which far exceeded the intravascular IR-820 signal of the contralateral, non-injected hind limb and was significantly elevated compared to the NS ($p<0.001$) and non-injured ($p<0.001$) groups. The paired difference represented a 2-fold increase in the signal intensity of the CTX injected hind limb over the non-injected hind limb. The paired difference remained significantly elevated through the 48 hour time points compared to both the NS ($p<0.001$) and non-injured groups ($p<0.001$). The paired difference in the CTX group was significantly elevated compared to baseline from the 1.5 through the 72 hour time points ($p\leq0.03$). These data suggest that capillary leak begins within 1.5 hours after injury and that ongoing leak or decreased clearance continues for as long as 72 hours.

To determine if an ongoing vascular leak was occurring days after CTX injury, a separate group of *Hairless*$^{SHK1/SHK1}$ mice received IR-820 i.p. 24 hours after CTX injection into the right hind limb, concurrent with NS injection into the left hind limb. NS injection into the contralateral hind limb was performed to determine the vascular leak that was attributable to the CTX rather than injury induced by the needle or fluid volume. In this experiment, signal intensity of the NS hind limbs (data not shown) was similar to the non-injected IR-820 kinetics (Figure 3A). Next, the paired difference between the CTX-injected right hind limb and the NS-control left hind limb was calculated (Figure 3C). The extravascular IR-820 signal peaked 48 hours after CTX injection (24 hours after IR-820 injection) and was similar to baseline by the 144 hour time point. In contrast to the 2-fold increase in signal intensity when IR-820 injection preceded CTX injection (Figure 3B), the signal intensity of the CTX limb was increased 40% over the NS limb when IR-820 was injected 24 hours after CTX injection. In combination, these data suggest that initially a large vascular leak occurs within

hours of injury, and a smaller but ongoing vascular leak occurs for at least 48 hours after injury.

IR-820 is a contrast agent for a multitude of diseased tissues

To determine whether IR-820 could be used as a contrast agent for tumors, a mixed strain mouse bearing a neck tumor was injected with IR-820 via tail vein and imaged 15 minutes later. Near-infrared fluorescence was seen in a distribution characteristic of a blood pool contrast agent (bare skin of paws, tail and highly vascular region of the nose) (Figure 4A), yet a very significant amount of signal emanated from the tumor mass (28.4% of total flux). Tumor histology consistent with lymphoma is shown in the inset. Small metastases, however, were difficult to visualize in similar experiments (data not shown).

To demonstrate the use of IR-820 for lymph node mapping, we injected IR-820 directly in a rhabdomyosarcoma tumor on the left foot of a transgenic *Myf6* $^{\text{ICNm/WT}}$ *Pax3* $^{\text{P3Fm/P3Fm}}$ *Trp53* $^{\text{F2-10/WT}}$ *Rb1* $^{\text{Flox/Flox}}$ mouse. Signal was present in the primary tumor as well as the ipsilateral popliteal lymph node and the proximal superficial inguinal lymph node (Figure 4B), as confirmed by necropsy. Histologically, the primary tumor was consistent with rhabdomyosarcoma (Figure 4B inset) but only the popliteal lymph node (which bore the highest fluorescence) contained metastatic tumor cells.

Thrombotic stroke is a non-oncological example of disordered vascular integrity. Thromboses re-route cerebral circulation causing regions of focal ischemia and potential damage to the blood-brain barrier (BBB) at the site of each thrombus. To assess whether BBB permeability could be imaged *in vivo*, non-invasive, photothrombotic vascular occlusions were induced by irradiating a 1mm^2 circular region of the mouse cortex following tail injection of the photosensiting dye Rose Bengal (RB). When RB dye is excited with green light (543 nm), the dye fluoresces red and the brain blood vessels are easily observed using optical microscopy. However, when RB is excited for prolonged periods, singlet oxygen molecules are generated, locally damaging the blood vessel walls and inducing thrombosis. BBB permeability was tested by tail-vein injection of IR-820; at various periods subsequent to the initial photothrombosis. IR-820 leakage from the intravascular compartment was interpreted to reflect increased BBB permeability induced by the photothrombotic stroke. As expected for damaged blood vessels, significant IR-820 fluorescence was observed in regions of the cortex that were in close proximity to photothrombosed area (Figure 4C). Extravasation of the dye occurred over an area much larger than the initial lesion (Figure 4C Inset). However, IR-820 fluorescence was not observed in control mice that underwent identical procedures without tail vein injections of RB (data not shown).

Discussion

IR-820 is a novel and inexpensive near-infrared blood pool contrast agent ($\lambda_{\text{excitation}}$ 710 nm, $\lambda_{\text{emission}}$ 820 nm) with enhanced biological fluorescence attributable to albumin binding in the serum. Clearance is hepatobiliary and is near complete (99%) 8 days after intraperitoneal or intravenous injection. IR-820 clearance is similar to the clearance of albumin ($t_{1/2}$= 35 hours; 5 half lives =7.3 days)11. We speculate that the slight difference in intravenous versus intraperitoneal kinetics may be attributable to increased portal/ hepatobiliary clearance with intraperitoneal injection. By either route of delivery, near complete clearance (99%) occurred after 8 days of IR-820 administration. Furthermore, we have shown that IR-820 accumulates in injured muscle, and we also demonstrate that IR-820 is sequestered in several disease conditions with increased vascular permeability, including tumors and stroke.

Optical contrast agents are ideally suited to whole-animal studies. In the near-infrared electromagnetic spectrum, tissue absorption and scattering are at a minimum, thereby providing a high level of signal penetration. This region of spectra is well established to have the minimum penetration due to the optical properties of the oxy- and deoxy-hemoglobin12. Disadvantages of optical imaging in general include dampening of the signal through skin that is pigmented or contains hair. However, hair removal by clipping or depilatory agents can facilitate the use of IR-820 in a diverse array of animal species. To demonstrate the use of IR-820 to monitor tissue injury and recovery over time, we utilized a well-characterized cardiotoxin injury model10. CTX contains lytic factors whose primary mechanism of action is forming pores that depolarize and degrade the muscle plasma membrane13. CTX injection results in muscle necrosis followed by an inflammatory and regenerative response similar to the injury-repair response observed in muscle following an ischemic injury10,14. IR-820 injected into the intraperitoneal space is absorbed into the vascular system, binds to serum albumin, and emits a reproducible intravascular signal as demonstrated by the non-injured group and the non-injected hind limbs of the CTX group and NS group. Our findings demonstrate an increased IR-820 signal in muscle after both mild (NS injection) and severe (CTX injection) injury and that the severity of injury influences the intensity of the IR-820 signal. CTX causes muscle necrosis with disruption of the capillary network13. The intravascular, albumin-bound IR-820 leaked into the CTX-injured muscle immediately post-injection presumably due to increased permeability from disruption of the endothelial barrier function. Normally, the endothelial barrier function is maintained by a continuous membrane composed of semi-permeable endothelial cells15. Disruption of the endothelial barrier function results in extravasation of fluid and proteins, including albumin, leading to tissue edema16 and in the present study, an extravascular IR-820 signal. In addition, endothelial dysfunction from neighboring regions of intact muscle may have also contributed to extravasation of IR-820 bound albumin. Consistent with the histology demonstrating diffuse myonecrosis, the IR-820 signal difference peaked at 1 hour after CTX injection and remained elevated for several days. The paired difference in the CTX-injured group remained significantly increased until the 72 hour time point, which histologically corresponded to macrophage infiltration into the injured muscle10. Macrophages phagocytize necrotic myofibers19 and may also assist in the clearance of extravascular albumin, thus decreasing the IR-820 signal. Resolution of the extravascular IR-820 signal may result from a combination of vascular leak cessation as well as effective IR-820-bound albumin removal from the extravascular space. A continued, multi-day IR-820 leak was demonstrated by injecting IR-820 24 hours subsequent to CTX injection. Thus, the extravascular IR-820 signal is likely determined by the kinetics of the vascular leak versus IR-820-bound albumin removal. Interestingly, CTX injury did not induce any systemic increase in vascular permeability, as the absolute signal intensity of the control limbs was remarkably similar in non-injured, NS and CTX injected mice. Thus, the CTX model provides an example of how timing of IR-820 can reveal complementary information on the time course of capillary leak as well as the clearance of interstitial fluid.

In summary, IR-820 is an effective, low cost alternative to other commercial blood pool contrast agents20. This near-infrared contrast agent is ideally suited to preclinical applications requiring qualitative and quantitative assessment of injured tissue as well as diseased tissue with capillary leak, including tumors and stroke.

Acknowledgments

Charles Keller is a member of the UTHSCSA Cancer Therapy and Research Center. (P30 CA 54174). Supported in part by HL090196(COM), HL074236 and the Veterans Administration (PKS). We thank Dr. Brian P. Rubin for histological evaluation of the murine sarcoma.

References

1. Sevick-Muraca EM, Houston JP, Gurfinkel M. Fluorescence-enhanced, near infrared diagnostic imaging with contrast agents. Curr Opin Chem Biol. 2002; 6:642–50. [PubMed: 12413549]
2. Nomoto H, Shiraga F, Yamaji H, et al. Evaluation of radial optic neurotomy for central retinal vein occlusion by indocyanine green videoangiography and image analysis. Am J Ophthalmol. 2004; 138:612–9. [PubMed: 15488789]
3. Hori T, Yagi S, Iida T, et al. Stability of cirrhotic systemic hemodynamics ensures sufficient splanchnic blood flow after living-donor liver transplantation in adult recipients with liver cirrhosis. World J Gastroenterol. 2007; 13:5918–25. [PubMed: 17990357]
4. Cao Y, Pan C, Balter JM, et al. Liver function after irradiation based on computed tomographic portal vein perfusion imaging. Int J Radiat Oncol Biol Phys. 2008; 70:154–60. [PubMed: 17855011]
5. Nahrendorf M, Sosnovik DE, Waterman P, et al. Dual channel optical tomographic imaging of leukocyte recruitment and protease activity in the healing myocardial infarct. Circ Res. 2007; 100:1218–25. [PubMed: 17379832]
6. Osei-Owusu P, Sun X, Drenan RM, et al. Regulation of RGS2 and second messenger signaling in vascular smooth muscle cells by cGMP-dependent protein kinase. J Biol Chem. 2007; 282:31656–65. [PubMed: 17681944]
7. Hawrysz DJ, Sevick-Muraca EM. Developments toward diagnostic breast cancer imaging using near-infrared optical measurements and fluorescent contrast agents. Neoplasia. 2000; 2:388–417. [PubMed: 11191107]
8. Stoye JP, Fenner S, Greenoak GE, et al. Role of endogenous retroviruses as mutagens: the hairless mutation of mice. Cell. 1988; 54:383–91. [PubMed: 2840205]
9. Thurmond RL, Gelfand EW, Dunford PJ. The role of histamine H1 and H4 receptors in allergic inflammation: the search for new antihistamines. Nat Rev Drug Discov. 2008; 7:41–53. [PubMed: 18172439]
10. Ochoa O, Sun D, Reyes-Reyna SM, et al. Delayed angiogenesis and VEGF production in CCR2-/- mice during impaired skeletal muscle regeneration. Am J Physiol Regul Integr Comp Physiol. 2007; 293:R651–61. [PubMed: 17522124]
11. Chaudhury C, Mehnaz S, Robinson JM, Hayton WL, et al. The major histocompatibility complex-related Fc receptor for IgG (FcRn) binds albumin and prolongs its lifespan. J Exp Med. 2003; 197:315–22. [PubMed: 12566415]
12. Cerussi AE, Berger AJ, Bevilacqua F, et al. Sources of absorption and scattering contrast for near-infrared optical mammography. Acad Radiol. 2001; 8:211–8. [PubMed: 11249084]
13. Harris JB. Myotoxic phospholipases A2 and the regeneration of skeletal muscles. Toxicon. 2003; 42:933–45. [PubMed: 15019492]
14. Contreras-Shannon V, Ochoa O, Reyes-Reyna SM, et al. Fat accumulation with altered inflammation and regeneration in skeletal muscle of CCR2-/- mice following ischemic injury. Am J Physiol Cell Physiol. 2007; 292:C953–67. [PubMed: 17020936]
15. Matsuda N, Hattori Y. Vascular biology in sepsis: pathophysiological and therapeutic significance of vascular dysfunction. J Smooth Muscle Res. 2007; 43:117–37. [PubMed: 17928746]
16. Stevens T, Garcia JG, Shasby DM, et al. Mechanisms regulating endothelial cell barrier function. Am J Physiol Lung Cell Mol Physiol. 2000; 279:L419–22. [PubMed: 10956614]
17. Vallet B, Wiel E. Endothelial cell dysfunction and coagulation. Crit Care Med. 2001; 29:S36–41. [PubMed: 11445732]
18. Chen SE, Gerken E, Zhang Y, et al. Role of TNF-{alpha} signaling in regeneration of cardiotoxin-injured muscle. Am J Physiol Cell Physiol. 2005; 289:C1179–87. [PubMed: 16079187]
19. Pimorady-Esfahani A, Grounds MD, McMenamin PG. Macrophages and dendritic cells in normal and regenerating murine skeletal muscle. Muscle Nerve. 1997; 20:158–66. [PubMed: 9040653]
20. Alencar H, Mahmood U, Kawano Y, et al. Novel multiwavelength microscopic scanner for mouse imaging. Neoplasia. 2005; 7:977–83. [PubMed: 16331883]

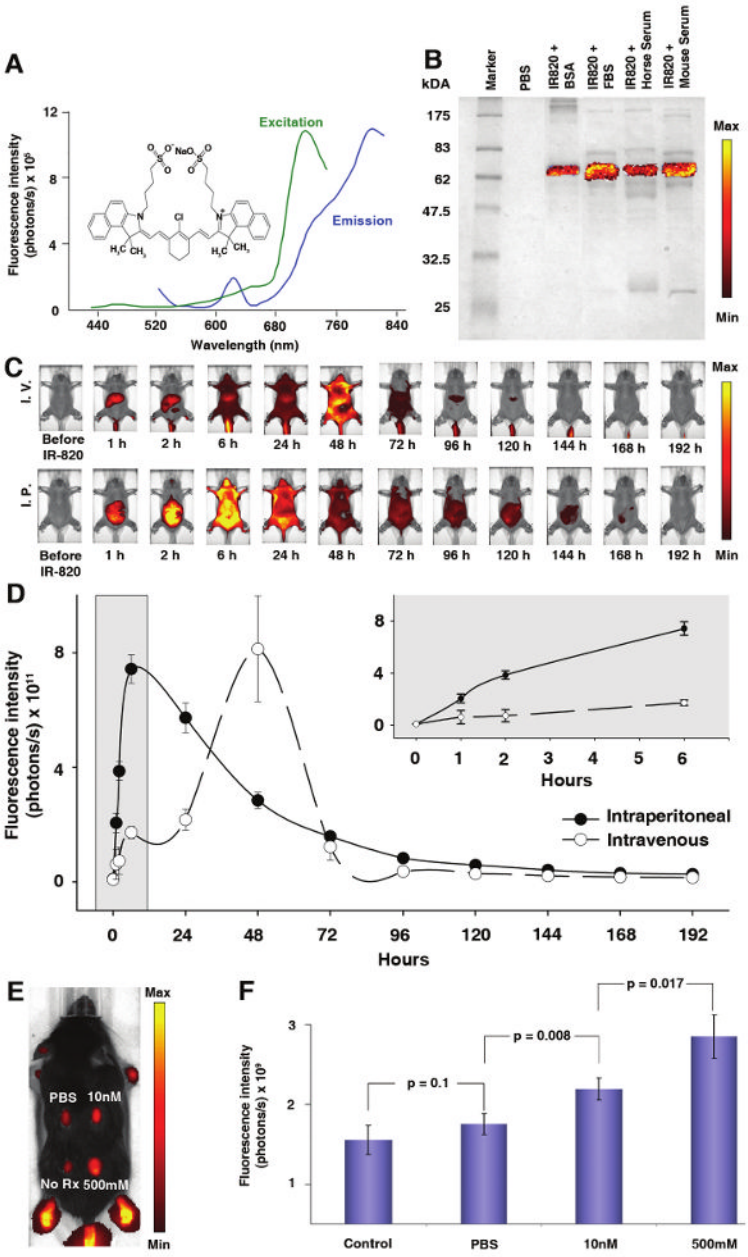

Figure 1.

IR-820 is a commercially available optoelectronic chemical with promising applications in biological (preclinical) optical imaging. (**A**) Spectra for free IR-820 reveal excitation and emission peaks at 710 nm and 820 nm respectively. Inset shows the molecular structure of IR-820. (**B**) IR-820 and protein interaction visualized using 10% SDS PAGE stained with Coomassie Blue shows fluorescence signal in all serum samples at a size similar to bovine serum albumin. The scale bar ranges from 1×10^6 to 1×10^7 photons/s/cm^2/steradian. (**C**) Whole body pharmacokinetics of IR-820 in hairless mice. Mice injected with 100 μl of IR-820 contrast agent intravenously through tail vein (top set) and intraperitoneal injection (bottom set). For both sets, first image prior to injection of IR-820, time thereafter in reference to IR-820 injection. The images are displayed with a minimum – maximum scale of 4×10^8 to 4×10^9 photons/s/cm^2/steradian. (**D**) The animals were serially imaged for 8

days with considerable decrease in signal at 3 days after injection. Error bars, s.d.; n=4 mice/group. (**E**) Vascular permeability in a dose-dependent manner was increased by intradermal injection of histamine (0, 10 nM or 500 mM, each in a volume of 50 μl) in PBS. The left caudal thorax received no injection. IR-820 was injected intravenously and imaging was performed in triplicate on a single mouse 30 minutes after histamine injection. The image is adjusted at a minimum – maximum scale of 4×10^9 to 4×10^{10} photons/s/cm^2/steradian. (**F**) Quantitative fluorescence signal of Figure 1E shows an increase in signal from the histamine injected sites due to vasodilation of the tissues. Error bars, s.d.

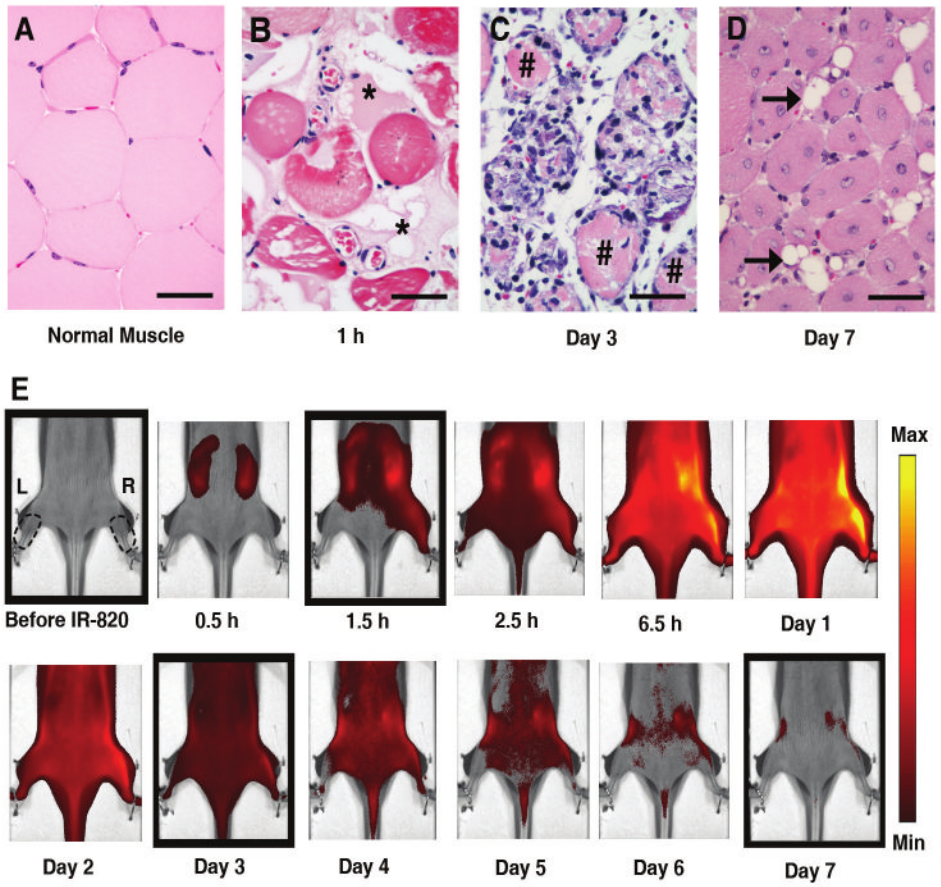

Figure 2.

Histology of cardiotoxin-induced injury and kinetics of IR-820 distribution. Representative microscopic appearance of normal (**A**) and injured muscle obtained at 1 hour (**B**) 3 days (**C**) or 7 days (**D**) following cardiotoxin treatment; * shows location of acellular protein; # demonstrates location of necrotic myofiber; horizontal arrow points to adipocyte; scale bar, 50 μm, hematoxylin and eosin. (**E**) *Hairless*$^{SKH1/SKH1}$ mouse serial images after injury on right (R) hind limb with intramuscular cardiotoxin injection and no injection on the left (L) hind limb. The images are displayed with a minimum – maximum scale of 4×10^8 to 4×10^9 photons/s/cm^2/steradian. Right and left regions of interest are shown as dotted lines. First image prior to intraperitoneal injection of IR-820, time thereafter in reference to IR-820 injection, cardiotoxin injected 0.5 hour after IR-820 injection. The boxed images correspond to the histology pictures in Figure 2A-D from left to right.

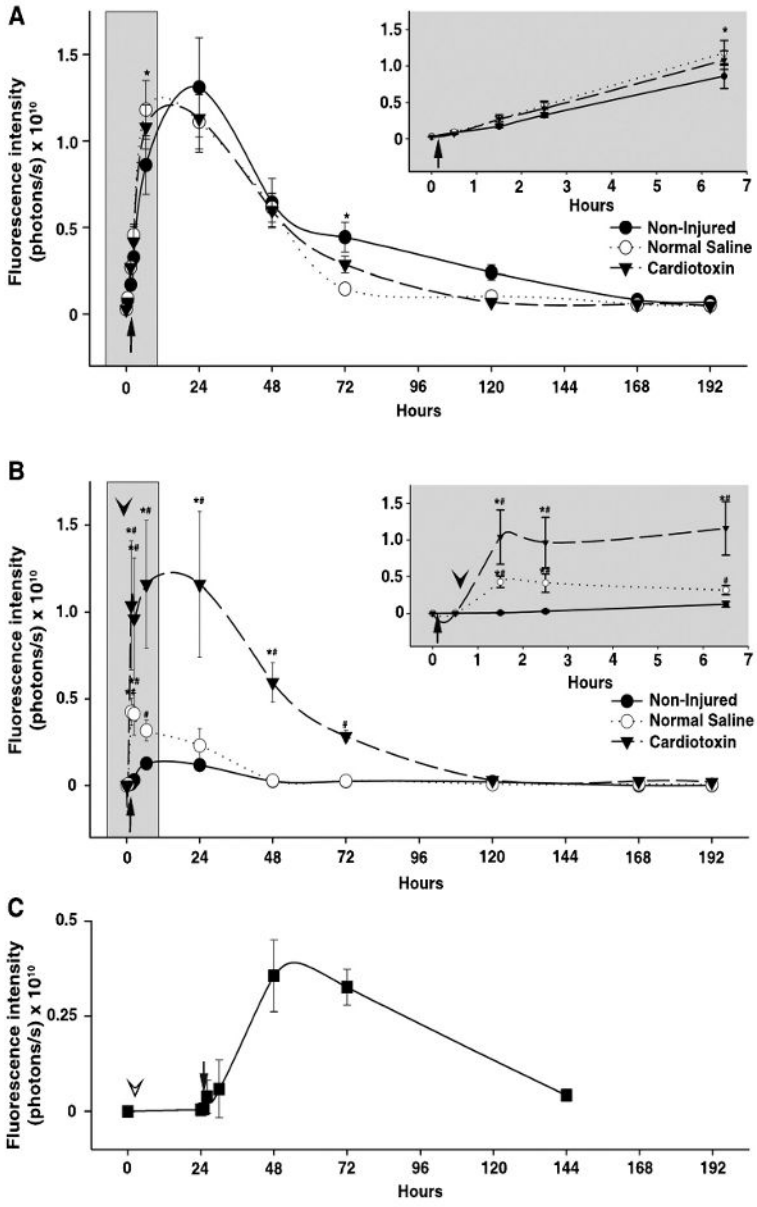

Figure 3.

Kinetics of IR-820 in normal and injured lower limb muscle tissue of *Hairless*$^{SKH1/SKH1}$ mice. (**A**) The signal intensity plot of non-injected, left hind limbs. Inset graph demonstrates an expanded view of the early time points immediately following IR-820 injection. * denotes p≤0.03 in pairwise comparison between normal saline or cardiotoxin groups compared to the Non-injured group. Error bars, s.d.; n=3-4 mice/group. (**B**) Paired difference of injected hind limb and non-injected hind limb, time on x-axis measured after IR-820 injection (arrow); cardiotoxin or normal saline injection into the right hind limb denoted by the arrowhead. Inset graph demonstrates an expanded view of the early time points immediately following IR-820 and cardiotoxin or normal saline injection. * denotes p≤0.01 in pairwise comparison between groups. # denotes p≤0.03 for each time point within each group compared to baseline, defined as 0.5 hours after IR-820 injection and prior to cardiotoxin or normal saline injection. Error bars, s.d.; n=3-4 mice/group. (**C**) Ongoing vascular leak demonstrated by the paired difference of cardiotoxin (right) and normal saline

(left) injected hind limbs (arrowhead) followed by intraperitoneal IR-820 injection (arrow) 24 hours later. Time on x-axis measured after cardiotoxin and normal saline injections. Error bars, s.d.; n=2 mice/group.

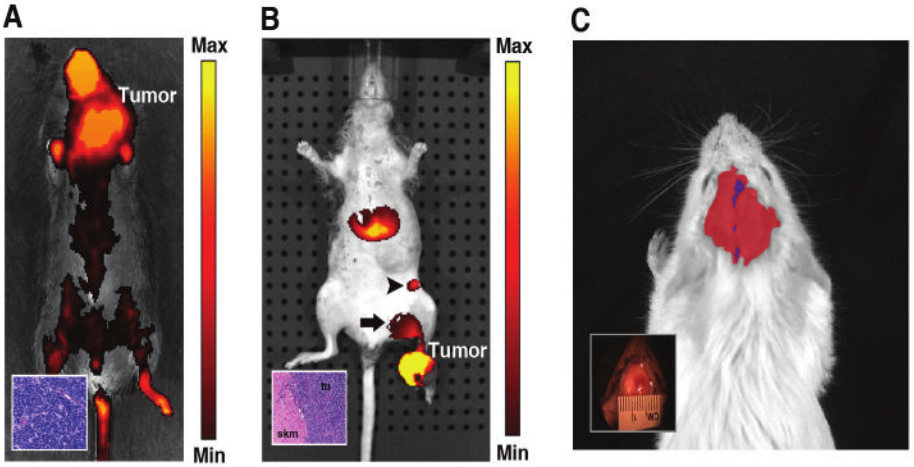

Figure 4.

In vivo imaging of diseased animals using IR-820. (**A**) A mouse bearing a neck tumor was imaged 15 minutes after injection of 100 μl of IR-820 intravenously through tail vein injection. A large portion (28.4% of total) of the IR-820 fluorescence was concentrated in the viable solid tumor region. The inset shows the histology which was consistent with lymphoma. The image has been displayed at a minimum – maximum scale of 3×10^8 to 2×10^9 photons/s/cm^2/steradian. (**B**) 100 μl of IR-820 was administered directly into the foot tumor of a transgenic *Myf6* $^{\text{ICNm/WT}}$ *Pax3* $^{\text{P3Fm/P3Fm}}$ *Trp53* $^{\text{F2-10/WT}}$ *Rb1* $^{\text{Flox/Flox}}$ mouse and imaged 24 hours after injection. Fluorescence signal is present at the tumor site as well as popliteal (arrow) and inguinal (arrow head) lymph nodes. Histology demonstrates rhabdomyosarcoma tumor cells adjacent to normal skeletal muscle (inset). tu stands for tumor, skm stands for skeletal muscle. The image is thresholded at a minimum – maximum scale of 5×10^8 to 1×10^9 photons/s/cm^2/steradian. (**C**) IR-820 contrast agent was given via tail vein injection into a mouse after induction of a thrombotic stroke. Blue region shows the site of the stroke and red region shows the swelling in the area of tissue injury caused by the stroke. The inset shows the gross picture of mouse with stoke. A minimum – maximum scale of 8×10^8 to 6×10^9 photons/s/cm^2/steradian has been used to display the image.